JNeurosci
THE JOURNAL OF NEUROSCIENCE

Research Articles: Development/Plasticity/Repair

Longitudinally Mapping Childhood Socioeconomic Status Associations with Cortical and Subcortical Morphology

Cassidy L. McDermott[a], Jakob Seidlitz[a], Ajay Nadig[a], Siyuan Liu[a], Liv S. Clasen[a], Jonathan D. Blumenthal[a], Paul Kirkpatrick Reardon[a], François Lalonde[a], Deanna Greenstein[b], Raihaan Patel[c], M. Mallar Chakravarty[c,d], Jason P. Lerch[e] and Armin Raznahan[a]

[a]*Developmental Neurogenomics Unit, Human Genetics Branch, National Institute of Mental Health, Bethesda, MD 20892*

[b]*Experimental Therapeutics and Pathophysiology Branch, National Institute of Mental Health, Bethesda, MD 20892*

[c]*Cerebral Imaging Centre, Douglas Mental Health University Institute, McGill University, Montreal, QC, Canada H4H 1R3*

[d]*Department of Psychiatry, McGill University, Montreal, QC, Canada H3A OG4*

[e]*Department of Medical Biophysics, University of Toronto, Toronto, ON, Canada M5G 1L7*

https://doi.org/10.1523/JNEUROSCI.1808-18.2018

Received: 13 July 2018

Revised: 31 October 2018

Accepted: 16 November 2018

Published: 26 December 2018

Author contributions: C.L.M., J.S.nd A.R. designed research; C.L.M., S.L., P.R., D.G.nd A.R. analyzed data; C.L.M. wrote the first draft of the paper; C.L.M., J.S., A.N.nd A.R. edited the paper; C.L.M. and A.R. wrote the paper; L.C., J.B.nd F.L. performed research; R.P., M.M.C.nd J.L. contributed unpublished reagents/analytic tools.

Conflict of Interest: The authors declare no competing financial interests.

The authors wish to thank the participants and families who took part in this study. This work was supported by the Intramural Research Program of the NIMH (1ZIAMH002949-01) under protocol NCT00001246.

Correspondence: Dr. Armin Raznahan, Developmental Neurogenomics Unit, NIMH, National Institutes of Health, 10 Center Drive, Room 4D18, MSC 1367, Bethesda, MD 20892. Phone: 301-435-7927. Email: raznahana@mail.nih.gov

Cite as: J. Neurosci 2018; 10.1523/JNEUROSCI.1808-18.2018

Title: Longitudinally Mapping Childhood Socioeconomic Status Associations with Cortical and Subcortical Morphology

Abbreviated Title: Socioeconomic Status and Brain Development

Cassidy L. McDermott[a], Jakob Seidlitz[a], Ajay Nadig[a], Siyuan Liu[a], Liv S. Clasen[a], Jonathan D. Blumenthal[a], Paul Kirkpatrick Reardon[a], François Lalonde[a], Deanna Greenstein[b], Raihaan Patel[c], M. Mallar Chakravarty[c,d], Jason P. Lerch[e], Armin Raznahan[a]

[a]Developmental Neurogenomics Unit, Human Genetics Branch, National Institute of Mental Health, Bethesda, MD 20892

[b]Experimental Therapeutics and Pathophysiology Branch, National Institute of Mental Health, Bethesda, MD 20892

[c]Cerebral Imaging Centre, Douglas Mental Health University Institute, McGill University, Montreal, QC, Canada H4H 1R3

[d]Department of Psychiatry, McGill University, Montreal, QC, Canada H3A OG4

[e]Department of Medical Biophysics, University of Toronto, Toronto, ON, Canada M5G 1L7

Address correspondence to: Dr. Armin Raznahan, Developmental Neurogenomics Unit, NIMH, National Institutes of Health, 10 Center Drive, Room 4D18, MSC 1367, Bethesda, MD 20892.

Phone: 301-435-7927

Email: raznahana@mail.nih.gov

Number of pages: 38

Number of figures and tables: 5

Abstract word count: 205

Introduction word count: 650

Discussion word count: 1495

Conflict of Interest

The authors have no conflicts of interest to declare.

Acknowledgments

The authors wish to thank the participants and families who took part in this study. This work was supported by the Intramural Research Program of the NIMH (1ZIAMH002949-01) under protocol NCT00001246.

Abstract

Childhood socioeconomic status (SES) impacts cognitive development and mental health, but its association with human structural brain development is not yet well-characterized. Here, we analyzed 1243 longitudinally-acquired structural MRI scans from 623 youth (299 female/324 male) to investigate the relation between SES and cortical and subcortical morphology between ages 5 and 25 years. We found positive associations between SES and total volumes of the brain, cortical sheet, and four separate subcortical structures. These associations were stable between ages 5 and 25. Surface-based shape analysis revealed that higher SES is associated with areal expansion of (i) lateral prefrontal, anterior cingulate, lateral temporal, and superior parietal cortices and (ii) ventrolateral thalamic, and medial amygdalo-hippocampal sub-regions. Meta-analyses of functional imaging data indicate that cortical correlates of SES are centered on brain systems subserving sensorimotor functions, language, memory, and emotional processing. We further show that anatomical variation within a subset of these cortical regions partially mediates the positive association between SES and IQ. Finally, we identify neuroanatomical correlates of SES that exist above and beyond accompanying variation in IQ. While SES is clearly a complex construct which likely relates to development through diverse, non-deterministic processes, our findings elucidate potential neuroanatomical mediators of the association between SES and cognitive outcomes.

Significance Statement

Childhood socioeconomic status (SES) has been associated with developmental disparities in mental health, cognitive ability, and academic achievement, but efforts to understand underlying SES-brain relationships are ongoing. Here, we leverage a unique developmental neuroimaging dataset to longitudinally map the associations between SES and regional brain anatomy at high spatiotemporal resolution. We find widespread associations between SES and global cortical and subcortical volumes and surface area, and localize these correlations to a distributed set of cortical, thalamic, and amygdalohippocampal subregions. Anatomical variation within a subset of these regions partially mediates the positive relationship between SES and IQ. Our findings help to localize cortical and subcortical systems which represent candidate biological substrates for the known relationships between SES and cognition.

65 **Introduction**

66 Early brain development occurs within the context of each child's experiences and
67 environment, which vary significantly as a function of socioeconomic status (SES). Childhood
68 SES is typically measured by factors including parental income, education, and occupation
69 (Hollingshead, 1957; McLoyd, 1998), and has been associated with disparate outcomes in
70 mental health, cognitive development, and academic achievement (Brooks-Gunn and Duncan,
71 1997; Sirin, 2005; Noble et al., 2007; Reiss, 2013). These associations are thought to arise
72 through diverse causal pathways, including (i) direct SES-linked effects on cognitive and health
73 outcomes (Ritsher et al., 2001; Kendler et al., 2015), (ii) the capacity of mental health or
74 cognitive challenges to negatively impact SES (Tiikkaja et al., 2016), and (iii) factors that
75 simultaneously increase risk for lowered SES and cognitive difficulties (Trzaskowski et al., 2014;
76 Hill et al., 2016).

77 The robust epidemiological data connecting childhood SES to behavioral and cognitive
78 development have motivated recent neuroimaging studies aimed at mapping SES effects on
79 brain anatomy. SES has been positively associated with total grey matter volume, and less
80 consistently with white matter volume (Luby et al., 2013; Hair et al., 2015; Gianaros et al.,
81 2017), as well as with volume in regions of a priori interest, including the prefrontal cortex and
82 hippocampus (Jednoróg et al., 2012; Noble et al., 2012; Hanson et al., 2013; Luby et al., 2013;
83 Hair et al., 2015; Holz et al., 2015). Furthermore, a recent landmark study (Noble et al., 2015)
84 mapped spatial cross-sectional associations between socioeconomic factors and cortical surface
85 area. These studies suggest that observed associations between childhood SES and
86 neurodevelopmental outcomes may be centered on specific brain systems, and raise as yet

unresolved questions regarding when SES-neuroanatomy associations are established, whether they are predominantly cortical or subcortical, and how correlations between SES and neuroanatomy relate to accompanying variation in cognitive ability (Noble et al., 2007; Brito and Noble, 2014).

Here, we seek to build on the current understanding of SES and brain development in five key directions. First, to determine whether SES associations with neuroanatomy are developmentally dynamic or stable in this age range (Giedd et al., 1999), we model SES-brain associations in a longitudinal sample of 1243 structural neuroimaging scans from 623 healthy individuals ages 5 to 25. We combine two complementary approaches to analysis of longitudinal data: mixed models (Pinheiro et al., 2016), and direct analysis of intra-individual estimates of anatomical change computed from repeat scans. Second, we separately model SES associations with regional cortical thickness (CT) and surface area (SA) – two biologically distinct phenotypes which together determine cortical volume (Raznahan et al., 2011). Findings remain sparse and mixed regarding the relative strength and spatial distribution of SES relations with SA and CT (Lawson et al., 2013; Noble et al., 2015). Third, we extend our analyses to assess the relation between SES and the anatomy of five major non-cortical structures (henceforth "subcortical" structures) using multi-atlas methods that provide both bulk volume estimates and spatially fine-grained measures of shape. Simultaneous examination of SES associations with cortical and subcortical anatomy is critical given evidence that these brain systems function (Redgrave et al., 2010), develop (Raznahan et al., 2014) and connect (Draganski et al., 2008) in a topographically organized manner. Fourth, we formally characterize functional associations of those cortical regions that correlate with SES using the Neurosynth platform for

meta-analysis of neuroimaging data (Yarkoni et al., 2011). Finally, given previously noted positive associations between SES and cognitive performance and the potential of brain anatomy to vary as a function of cognitive ability (Walhovd et al., 2016), we probe the complex associations between SES, neuroanatomy, and cognition through two methods that have been used separately in previous literature: (i) including IQ as a covariate in models of SES effects on neuroanatomy (Noble et al., 2012; Lawson et al., 2013) and (ii) assessing whether structural phenotypes correlated with SES mediate the relation between SES and IQ (Hair et al., 2015; Noble et al., 2015).

Materials and Methods

Participants

This study includes a longitudinal sample of 1243 structural magnetic resonance imaging (sMRI) brain scans from 623 healthy children and adolescents between 5 and 25 years old (Table 1). Participants were recruited through local advertisement for a study of typical brain development conducted at the National Institute of Mental Health Intramural Research Program between 1990 and 2010. Participants were screened and excluded on the basis of a history of mental health treatment, use of psychiatric medication, enrollment in special services at school, or diagnosis of any medical condition known to affect the nervous system. The research protocol was approved by the institutional review board at the National Institute of Mental Health, and written informed consent or assent was obtained from all children who participated in the study, as well as consent from their parents if the child was under the age of 18.

131

132 *Socioeconomic Status*

133 Childhood socioeconomic status (SES) was quantified using the Amherst modification of
134 the Hollingshead two-factor index (Hollingshead, 1957; Watt, 1976). Parental education and
135 occupation were each coded on a 7-point scale, and these two values were used to derive and
136 record a single SES score that was used for analyses. When education and occupation were
137 reported for two parents, the highest SES was used. In the resulting index, children from the
138 most advantaged families receive the lowest Hollingshead score of 20, while children from the
139 most disadvantaged families receive the highest Hollingshead score of 134. For ease of
140 interpretation, we refer to SES variation using conventional directionality, such that "higher
141 SES" refers to a lower Hollingshead score. Accordingly, reported positive associations with SES
142 in the manuscript indicate variables that increase in value with greater SES, and are thus
143 negatively correlated with Hollingshead score. In graphical representation of such associations,
144 x-axis scales for SES are reversed, such that right-most values index the highest SES levels (i.e.,
145 lowest Hollingshead scores).

146

147 *General Cognitive Ability*

148 Full-Scale IQ was estimated for each child in the sample using an age-appropriate
149 Wechsler scale. The majority (*N* = 562) of children received the Wechsler Abbreviated Scale of
150 Intelligence (Wechsler, 1999), and other scales used include the WAIS-R, WISC-R and WISC-III,
151 and the WPPSI and WPPSI-III. Of the 344 individuals with repeat assessments, only 60 had IQ

measures within one year of at least two scans. We therefore used the most recent complete IQ measurement for each individual.

Image acquisition and processing

All sMRI scans were T1-weighted images collected on the same 1.5 T General Electric SIGNA scanner with contiguous 1.5 mm axial slices using a 3D spoiled-gradient recalled-echo sequence (echo time = 5ms; repetition time = 24ms; flip angle = 45°; acquisition matrix = 256 × 192; number of excitations = 1; field of view = 24 cm). All scans passed visual assessment for motion artifact prior to processing.

Native sMRI scans were submitted to the CIVET 1.1.10 pipeline for automated morphometric analysis (Ad-Dab'bagh et al., 2006). The CIVET pipeline uses a validated neural net approach to voxel classification to calculate grey matter and white matter volume estimates (Zijdenbos et al., 2002; Cocosco et al., 2003) after initial correction of images for radiofrequency intensity non-uniformities (Collins et al., 1994; Sled et al., 1998). Following tissue classification, each image was fitted with two deformable mesh models to identify the inner and outer surface of cortical grey matter, and these surfaces were used to calculate cortical thickness and surface area at 40,962 vertices on each cortical hemisphere as previously described (MacDonald et al., 2000; Raznahan et al., 2013).

Subcortical segmentation and surface extraction were completed automatically using the MAGeT Brain algorithm (Chakravarty et al., 2013; Raznahan et al., 2014). Scans were first registered to the ICBM 152 template and corrected for radiofrequency intensity non-uniformities (Collins et al., 1994; Sled et al., 1998). For the striatum, thalamus, and pallidum,

the segmentation atlas was created using a 3D reconstruction of serial histological data, warped to an MRI-based template (Chakravarty et al., 2006). The MAGeT pipeline then customized this atlas to 21 randomly selected subjects within the sample. All 1243 scans were then warped to this set of templates, providing a set of 21 candidate subcortical segmentations for each scan. For the hippocampus and amygdala, five reference atlases were generated from high resolution and contrast T1 and T2 weighted images from three males and two females using a 3T scanner with final super-sampled isotropic voxel dimensions of 0.3 mm (Wood, 2011). The MAGeT pipeline again created automated segmentation atlases for 21 randomly selected subjects, resulting in 105 possible segmentations (5 atlases x 21 templates) for each of the 1243 scans in our dataset. Each scan was labeled using the 21 striatum, thalamus and pallidum segmentations and the 105 hippocampus and amygdala segmentations, and the final segmentation was decided upon using a label voting procedure, such that the label occurring most frequently at each voxel was retained. These procedures provided estimates of total bilateral volume for the hippocampus, amygdala, thalamus, striatum and pallidum in each scan. All scans used for analysis passed visual quality control of these final subcortical segmentations to exclude visible segmentation errors of the five subcortical structures under study.

Surface-based representations of all five subcortical structures were then estimated on their respective atlases using a marching cubes algorithm (Lerch et al., 2008). Next, the nonlinear portions of the 21 transformations mapping each subject to the 21 input templates were concatenated and averaged across the template library to limit noise and increase precision and accuracy. These surface-based representations were warped to fit each template and each surface was warped to match each subject. This procedure yields 21 possible surface

196 representations per subject for the striatum, thalamus and pallidum, and 105 possible surface
197 representations for the hippocampus and amygdala, which were merged by estimating the
198 median coordinate representation at each location. Next, a third of the surface area of each
199 triangle forming the surface representation was assigned to each vertex within the triangle. The
200 surface area at each vertex is the sum of all such assignments from all connected triangles.
201 Finally, surface area values were blurred with a surface-based diffusion-smoothing kernel (5mm
202 for the amygdala, hippocampus, striatum and thalamus, and 3mm for the pallidum). This
203 processing stream generated surface area values for a total of 26,401 vertices across the five
204 subcortical structures in each scan.
205
206 *Experimental design and statistical analyses*
207 The effect of SES on each anatomical metric of interest was modeled using a linear
208 mixed effects model with sex and centered age as fixed effects covariates and each individual's
209 ID (to account for multiple longitudinal scans per individual) and family ID (to account for the
210 presence of dizygotic twin pairs and siblings in the sample) as nested random effects. All linear
211 mixed effects models discussed below were fitted using the R package nlme, version 3.1-128
212 (Pinheiro et al., 2016). Sex was treated as a categorical variable, coded as "M" or "F." SES and
213 age variables were both centered. Individual ID and family ID were specified as nested random
214 effects, and were fitted with random intercepts.
215 The decision to present core results with SES, sex and age as main effects was made
216 after first ruling out the presence of extensive interactions between these variables (i.e., SES ×
217 sex or SES × age interactions) in predicting structure or vertex-level anatomical variation effect

on each anatomical variable. For most structures, there was no significant interaction between fixed effects variables; the few cases where interactions were found will be noted in the text. Otherwise, anatomy for the *i*th family's *j*th individual's *k*th time point was modeled as follows:

$$Anatomy_{ijk} = Intercept + d_i + d_{ij} + \beta_{1A}(SES - mean\ SES) + \beta_{2A}(age - mean\ age) + \beta_{3A}(sex) + e_{ijk} \quad [A]$$

Dependent volumetric variables of interest included total brain volume (TBV – the sum of intracranial grey and white matter volume), total intracranial grey matter volume (GMV) and total intracranial white matter volume (WMV), the total bilateral volume of the cortex (CV), total cortical surface area (SA) and mean cortical thickness (CT), and total bilateral volume of each subcortical structure (i.e., "bulk" hippocampal, amygdalar, thalamic, striatal, and pallidal volumes). To aid comparison of the associations between SES and these diverse volumetric indices, we also estimated the standardized effect for each SES-volume association by re-running model [A] above after centering and scaling all variables so that the resulting β_1 coefficient would index the standard deviation shift in volume with one standard deviation increase in SES (i.e., a decrease of approximately 18 Hollingshead points).

Vertex-level anatomical variables of interest included cortical thickness and surface area at each of 80,962 cortical vertices and SA at each of 26,401 subcortical vertices (hippocampus, 1152 left/1215 right; amygdala, 1473 left/1405 right; thalamus, 3016 left/3108 right; striatum, 6450 left/6178 right; pallidum, 1266 left/1138 right). Vertex-specific β_1 coefficients were visualized on the corresponding cortical or subcortical surface after applying a false discovery rate (FDR) correction for multiple comparisons. FDR corrections were calculated separately

240 across the left and right cortical hemispheres and the left and right subcortical structures with *q*
241 (the expected proportion of false rejections of the null hypothesis) set to 0.05.

242 Finally, we probed the relation between SES, anatomical metrics, and cognition in two
243 ways. First, for all structures that showed a significant main effect of SES in model [A], we
244 tested the robustness of this effect to the inclusion of Full-Scale IQ as a covariate in the linear
245 mixed effects models. Separate main effects of SES and IQ were included after first ruling out
246 the presence of a significant SES by IQ interactive effect. For these analyses, anatomy for the *i*th
247 family's *j*th individual's *k*th time point was modeled as follows:

248

249 $Anatomy_{jk} = Intercept + d_i + d_{ij} + \beta_{1B}(SES - mean\ SES) + \beta_{2B}(IQ - mean\ IQ) + \beta_{3B}(age - mean\ age)$
250 $+ \beta_{4B}(sex) + e_{ijk}$ [B]

251

252 Linear age terms were used in models [A] and [B] after verifying that this simple
253 parameterization of age yielded identical SES findings to models run with age parameterized as
254 a non-linear spline (which could allow for non-linear age effects). Additionally, models [A] and
255 [B] were re-run for each anatomical metric within the subset of participants (n = 534) who self-
256 endorsed the federal race category of "white," and all main effects held.

257 To complement our mixed-effects models and further probe the nature of SES-anatomy
258 associations, we directly tested the relationship between SES and intra-individual change in
259 brain anatomy for the 344 individuals with more than one MRI scan. For each anatomical
260 variable, we calculated an annual rate of change for each individual. Anatomical change was
261 then modeled using a linear model with main effects of SES, mean scan age, and sex, and the

interaction between SES and mean scan age. The association between annual rate of change and SES was investigated for each of the anatomical variables considered in the mixed models above: TBV, GMV, WMV, CV, total SA, mean CT, five subcortical volumes, and vertex-wise CT, cortical SA and subcortical SA.

Finally, we conducted mediation analyses to investigate the extent to which the global and vertex-wise structural associations with SES mediate the association between SES and IQ. For the mediation tests with a single global mediator, we used the Mediation package in R (Tingley et al., 2014), with SES as the independent variable (treatment) and Full-Scale IQ as the dependent variable. The *mediate()* function estimates the average causal mediation effect (ACME) and the average direct effect (ADE), which together sum to the total effect of the treatment (i.e., SES) on the outcome (i.e., IQ). The proportion mediated, which we report, represents the size of the ACME relative to the total effect. Within the map of cortical vertices that showed a significant association with SES, we tested the mediating role of each vertex using the MultiMed package in R (Boca and Sampson, 2014), which implements a permutation approach with joint correction to test multiple mediators simultaneously.

Interpretation of Anatomical Results

To systematically investigate the functional implications of SES effects, we submitted the MNI coordinates of peak SES effects on surface area and cortical thickness to Neurosynth (Yarkoni et al., 2011). Neurosynth is an online platform that extracts and synthesizes brain activation patterns and psychological terms across >11,000 functional neuroimaging publications. It can be used to generate correlations between the meta-analytic co-activation

map for a given point of interest in the brain and each of the terms in the Neurosynth database. Using Neurosynth, we identified cognitive and psychological terms that frequently co-occur in the literature with functional activations similar to the observed pattern of SES effects on cortical morphology.

Results

Participant Characteristics

Participant characteristics are detailed in Table 1. Hollingshead SES in our sample ranged from a high of 20 to a low of 95 after 3 scans from individuals with exceptionally low SES scores (Hollingshead SES = 115, $|z\text{-}score| > 4$) were removed. The complete Hollingshead scale ranges from 20 to 134, and approximately one-quarter of our 623 participants received the highest SES score of 20 (indicating that one or both of their parents received a graduate professional degree and employment in the highest occupation category). Thus, our sample's distribution of Hollingshead scale scores does not capture the most severely socioeconomically disadvantaged children, and it is relatively enriched for children with highly-educated and highly-employed parents. Throughout the text below, SES is referred to using conventional directionality, such that "higher SES" refers to a lower Hollingshead score, and reported positive associations with SES are thus negatively correlated with Hollingshead score. Within the cross-sectional sample of 623 individuals, SES and IQ were significantly, positively correlated, $r(621) = 0.31$, $p < 0.001$.

SES and Measures of Brain Volume

We found a strong positive association between SES and total brain volume (β_{1A} = 1217.0, $p < 0.001$). A positive association with SES was also seen for total white and grey matter volumes, as well as for total volume of the cortical sheet (Table 2). Separate examination of the two determinants of cortical volume identified a strong positive association between SES and total cortical surface area (β_{1A} = 144.1, $p < 0.001$), and a weaker positive association between SES and mean cortical thickness (β_{1A} = 0.00086, p = 0.01). Greater SES was also significantly associated with greater bilateral volume of all subcortical volumes examined except the pallidum (Table 2). Analysis of standardized effect sizes for SES associations with regional brain volumes revealed that SES was most strongly related to total brain volume and total surface area, such that a standard deviation increase in SES was associated with a 0.17 SD increase in each of these metrics (Figure 1A). Among subcortical structures, SES had the greatest effect on thalamic volume, such that a standard deviation increase in SES was associated with a 0.15 SD increase in thalamic volume (Figure 1A).

These above associations between SES and brain anatomy were all stable between ages 5 and 25, and comparable between males and females, with two exceptions: (i) the association between SES and total cortical surface area was modified by sex, such that there was a stronger SES effect on surface area for males than females (SES × sex interaction effect: $\beta_{interaction}$ = 122.2, p = 0.019; SES main effects: $\beta_{1A,MALES}$ = 198.7, $p < 0.001$/$\beta_{1A,FEMALES}$ = 77.6, p = 0.066), and (ii) the association between SES and hippocampal volume was modified by age such that the effect of SES on hippocampal volume grows with age (SES × age interaction effect: $\beta_{interaction}$ = 0.19, p = 0.003).

SES and Cortical Morphology

After establishing that SES was associated with total surface area and mean cortical thickness (Table 2), we tested for regional specificity of these associations through vertex-level analysis of SES associations at 80,962 points (vertices) across the cortical sheet. Vertex-level analyses established that the robust association between greater SES and greater total cortical SA was underpinned by statistically-significant positive associations between SES and regional SA within a distributed set of largely bilateral cortical areas including the lateral prefrontal, anterior cingulate, lateral temporal and superior parietal lobule regions (Figure 1B, 3). Associations between SES and vertex-level SA were not significantly modified by age or sex after correction for multiple comparisons.

Associations between SES and regional cortical thickness were much more localized than observed for regional SA. Specifically, we identified a single locus of significant positive association between SES and CT in the right supramarginal gyrus (3).

SES and Subcortical Morphology

We investigated the spatial specificity of observed associations between SES and bilateral subcortical volumes by modeling surface area at each vertex across the surface of the hippocampus, amygdala, thalamus, and striatum (Figure 1C). Hippocampal effects were concentrated bilaterally on the medial surface, and neighboring medial surfaces of the right amygdala also showed a significant positive association with SES. The association between SES and thalamic surface area was localized primarily to the ventral posterior and ventral lateral

thalamus. No other subcortical structures showed statistically significant shape associations with SES after correcting for multiple comparisons across vertices.

SES and Intra-individual Anatomical Change

To complement our mixed model analyses and directly model intra-individual change, we further investigated the relationships between SES and annual rate of anatomical change of each of the cortical and subcortical metrics discussed above. Among the 344 individuals with more than one MRI scan, there was no significant relationship between SES and change in any of the global anatomical metrics (TTV, GMV, WMV, CV, total SA, mean CT, or any subcortical volume). These results are fully consistent with the previously noted lack of significant SES × age interactive effect on any global anatomical metric, with the sole exception of findings for hippocampal volume. Results from analyses of intra-individual change and from mixed-model analysis were also largely consistent for vertex-level measures of cortical surface area and thickness: both analytic approaches suggested that age does not modulate SES effects on thickness or surface area across most of the cortical sheet, or on area across subcortical surfaces. We observed two, spatially-limited, exceptions to this convergence between analytic techniques, in that analysis of intra-individual change uniquely identified, (i) a statistically-significant negative relationships between SES and cortical thickness change in the left middle temporal gyrus and the left superior parietal lobule, after FDR correction, and (ii) statistically-significant, negative relationship between SES and surface area change in a single locus on the left dorsal thalamus. A figure showing results of the vertex-wise change analyses is available on FigShare (McDermott, 2018).

Separating Main Effects of SES and IQ on Anatomy

Because of the noted strong association between SES and IQ (Figure 2A), we next re-ran linear mixed-effects models with Full-Scale IQ as a covariate, in order to parse main effects of SES and cognition on neuroanatomy. We observed positive associations between IQ and all global measures of cortical and subcortical anatomy (Table 2). The main effect of SES on each global metric was reduced in magnitude by the addition of IQ to the model; for mean cortical thickness, bulk amygdalar volume, and bulk striatal volume, the main effect of SES was no longer significant (Table 2), although SES continued to show a significant positive association with TBV, GMV, WMV, CV, total cortical SA, and bilateral hippocampal and thalamic volumes after controlling for IQ. There were no significant SES x IQ interactive effects on any global metrics.

We next probed the spatial patterning of IQ versus SES main effects on cortical surface area. After FDR correction for multiple comparisons, childhood SES and IQ were both positively associated with regional cortical SA (Figure 2B). Specifically, when including IQ as a covariate, the main effect of SES was restricted to the bilateral superior parietal, right orbitofrontal, left inferior temporal, and bilateral medial prefrontal cortices. The main effect of IQ, in contrast, was localized to the left inferior and middle temporal, left inferior parietal, and left medial frontal regions. Strikingly, the regional maps of separate SES and IQ effects on cortical surface area together (Figure 2B) resemble the regional effects of SES when IQ is not included as a covariate (Figure 1B). In other words, the main effect of SES on cortical surface area appears to be separable into effects related to the strong IQ differences across SES, localized to the left-

lateralized perisylvian and medial prefrontal cortices, and SES-SA associations that are independent from associated variation in general cognitive ability, localized to bilateral parietal and frontal cortices.

Structural Measures Mediate the Association Between SES and IQ

In addition to testing the effects of IQ as a covariate in SES-brain associations, we also probed the relation between SES, cognition, and anatomy by examining whether any of the structural brain measures found to be significantly associated with SES might mediate the association between SES and IQ in our cross-sectional dataset of 623 individuals. Using the Mediate package in R (Tingley et al., 2014), we estimated the proportion of the total relation between SES and IQ that was accounted for by each anatomical mediator. Among global cortical measures, total brain volume (proportion mediated = 0.148, $p < 0.001$), grey matter volume (proportion mediated = 0.145, $p < 0.001$), white matter volume (proportion mediated = 0.077, $p < 0.001$), cortical volume (proportion mediated = 0.146, $p < 0.001$), total surface area (proportion mediated = 0.114, $p < 0.001$), and mean cortical thickness (proportion mediated = 0.049, $p = 0.01$), each partially mediated the relation between SES and IQ. Subcortical volumes also partially mediated the association (hippocampus, proportion mediated = 0.052, $p < 0.001$; amygdala, proportion mediated = 0.034; $p = 0.02$; thalamus, proportion mediated = 0.087; $p < 0.001$; striatum, proportion mediated = 0.033, $p = 0.01$).

Finally, we extended the mediation analysis to investigate whether there was a regional specificity to the partial mediation of SES and IQ by cortical and subcortical surface area. To do so, we submitted all of the vertices in each hemisphere that showed a significant association

with SES to a multiple mediation analysis using the MultiMed package in R (Boca and Sampson, 2014). Three cortical regions – all in the left hemisphere – showed significant mediation of the SES association with IQ: the middle temporal gyrus, supramarginal gyrus, and anterior cingulate cortex (Figure 2C). Notably, these largely overlapped with the cortical vertices that showed shared main effects of SES and IQ on surface area (regions in purple, Figure 2B).

Functional Implications of Anatomical Results

Coordinates of peak regional SES associations with cortical surface area and cortical thickness were submitted to Neurosynth (Yarkoni et al., 2011), a meta-analytic repository of structure-function relationships. The top five cognitive and psychological terms with the highest meta-analytic co-activation correlation coefficient *r* are displayed in 3, after redundant terms and anatomical terms were removed. This platform provided evidence that the spatial effects of SES are localized to regions preferentially associated with sensorimotor functions, as well as language, memory, and emotional processing, which have each been shown to exhibit SES differences (Farah et al., 2006; Noble et al., 2007; Kim et al., 2013b).

Discussion

Here, with a large, longitudinal, single-site neuroimaging sample, we both replicate and extend findings on the relation between childhood SES and structural brain anatomy in a number of key directions.

First, in line with previously replicated findings, we find that SES is positively associated with global brain measures including grey matter volume (Hanson et al., 2013; Luby et al., 2013;

436 Mackey et al., 2015; Gianaros et al., 2017), cortical surface area (Noble et al., 2015; Gianaros et
437 al., 2017), cortical thickness (Mackey et al., 2015; Noble et al., 2015) and hippocampal volume
438 (Noble et al., 2012, 2015; Luby et al., 2013; Hair et al., 2015). While previous findings regarding
439 white matter volume and amygdala volume have been mixed (Jednoróg et al. 2012; Luby et al.
440 2013; Noble et al. 2015; Gianaros et al. 2017), we identify significant positive SES associations
441 with both WMV and amygdala volume. We extend analyses of SES associations with subcortical
442 anatomy to provide the first evidence that greater childhood SES is associated with larger
443 bilateral volumes of the thalamus and striatum. The thalamic finding is especially notable given
444 reported associations between thalamic volume and cognitive performance (Van Der Werf et
445 al., 2001; Xie et al., 2012). Comparative analyses of SES associations using standardized effect
446 sizes ranks total cortical SA and bilateral thalamic volume as the morphometric properties of
447 the cortex and subcortex, respectively, that show the largest effect-size relations with SES.

448 It is of particular note that, with the exception of hippocampal volume, we found the
449 above noted SES associations with global cortical and subcortical anatomical metrics to be fixed
450 between ages 5 and 25. This conclusion was supported by two complementary analytic
451 approaches: mixed model testing for significant SES × age interactive effects, and direct analysis
452 of SES effects on intra-individual rates of anatomical change. Other cross-sectional studies with
453 age ranges similar to the population examined here have likewise reported limited or no SES ×
454 age interactions (Lawson et al., 2013; Noble et al., 2015); however, a longitudinal study of
455 children under the age of 4 found that SES disparities in GMV grow with age (Hanson et al.,
456 2013). These findings suggest that SES and age may interact differently across developmental
457 time, with developmentally-dynamic associations early in life, which subsequently stabilize.

458 Future longitudinal studies which bridge the gap between infancy and adolescence may help
459 clarify the temporal dynamics of SES associations with brain development.

460 Second, our study advances understanding of the neuroanatomical correlates of SES by
461 using surface-based algorithms to parse associations between SES and anatomy of the cortical
462 sheet. We observe SES associations with cortical surface area in a number of largely bilateral
463 regions including lateral prefrontal, anterior cingulate, lateral temporal, and superior parietal
464 lobule regions. These SES-surface area associations largely correspond to the map of
465 associations between parental education and cortical surface area presented by Noble and
466 colleagues (Noble et al., 2015). Functional interpretation with Neurosynth (Yarkoni et al., 2011)
467 suggests that the cortical regions we find to show morphological associations with SES are
468 preferentially involved in networks that underlie sensorimotor functions, as well as language,
469 memory, and emotional regulation.

470 Third, we provide the first systematic examination of SES associations with subcortical
471 shape, which indicates that variations in childhood SES are associated with focal differences in
472 hippocampal, amygdalar and thalamic anatomy (Figure 1C). Histological and functional
473 connectivity neuroimaging studies suggest that the ventral lateral and ventral posterior
474 thalamic nuclei are preferentially connected to frontoparietal cortical systems which subserve
475 primarily sensorimotor functions (Jones, 1985; Kim et al., 2013a). Strikingly, we also detect
476 strong associations between SES and surface area within these cortical targets of ventral
477 thalamic nuclei, suggesting that anatomical correlations of childhood SES variation may be
478 organized by the topography of cortico-subcortical connectivity.

Finally, we demonstrate convergent anatomical correlates of the strong relation between SES and IQ using two independent methods. Modeling the main effects of both IQ and SES on vertex-wise surface area reveals that the map of statistical SES effects can be fractionated into distinct SES and IQ effects. Additionally, we demonstrate that many of the anatomical correlates of SES significantly mediate the relation between SES and IQ. We expand upon previous results that found significant SES-cognition mediation by whole-brain surface area (Noble et al., 2015) by conducting cross-sectional mediation tests at each cortical vertex that had a significant SES-surface area association. Specifically, we find that vertices in the left middle temporal gyrus, supramarginal gyrus, and anterior cingulate – the same three regions that showed a main effect of IQ when controlling for SES – mediate the relation between SES and IQ. These three regions are known to be involved in language (Vannest et al., 2009) and cognitive control (Shackman et al., 2011).

A mediation analysis allows us to test one possible pathway between SES, brain anatomy, and cognition, and we show that SES may exert some of its effect on cognition by altering structural brain development, particularly in regions associated with language and learning. However, it is important to note that this pathway represents only one possible set of interactions between childhood environment, anatomy, and cognition. Farah (Farah, 2017) provides a succinct review of the main processes that may operate to exacerbate neural and psychological SES disparities: the social causation hypothesis suggests that the environmental conditions associated with different levels of SES influence brain structure and function, while the social selection hypothesis suggests that genetic factors in parents that both affect their cognition and predispose them to a certain SES are then transmitted to their children. These

processes likely both operate in concert and interact to some degree. Because of the inherent observational nature of studies of SES, it is difficult to determine to what extent the anatomical correlates of SES that we report here may reflect the shared genetic effects on SES and brain development versus direct effects of SES on brain development. Nevertheless, our findings help to pinpoint cortical and subcortical systems which represent candidate biological substrates for these diverse causal pathways.

Caveats and Future Directions

One important limitation of this sample is the composite nature of the Hollingshead 2-factor index of SES. The field has lately recognized the importance of differentiating between the effects of separate components of socioeconomic status (Duncan and Magnuson, 2012). A few studies have already begun to identify differential effects of parental education and family income on structural brain development (Lawson et al., 2013; Noble et al., 2015). However, when data collection for this sample began in the 1990s, the Hollingshead was selected for its widespread use and ease of measurement, and only the single, derived SES score was recorded initially. As future studies are designed it will be important to report on more nuanced factors that compose SES and may have unique effects on brain development and thus serve as specific targets for intervention.

It is also important to note that the subjects in this sample are not representative of the socioeconomic distribution in the United States. Sample composition is known to affect conclusions about the normative trajectory of brain development (LeWinn et al., 2017). Additionally, some studies have suggested that socioeconomic variables relate most strongly to

brain development among the most disadvantaged children (Noble et al., 2015), and the fact that we did not detect such a gradient may be due to our unrepresentative SES distribution. The average IQ of our subjects was also higher than the expected mean of 100 (Table 1); however, IQ is known to increase across generations in the general population, so the high mean IQ may be partially attributable to the use of the same IQ assessment across the multiple decades of this study (Flynn, 1987). Finally, most investigations of SES and brain development to date, including this study, have sampled from Western nations in general and the United States in particular. Further research is necessary to explore how SES associations with brain development play out across other nations and cultures. Although we cannot generalize across the socioeconomic, cognitive, or cultural spectrums, it is notable that we found detectible SES-linked differences in cognitive ability and structural brain development within a typically developing cohort lacking frank socioeconomic deprivation.

Conclusion

Childhood socioeconomic status is a complex construct that influences the physical and psychosocial environment in which a child develops. Here, we demonstrate regionally-specific associations between childhood SES and both cortical and subcortical morphology. Our findings inform ongoing efforts to clarify the spatiotemporal patterning of SES-related neuroanatomical variation and its relation to cognitive outcomes such as IQ. Definition of these neuroanatomical associations may ultimately provide candidate biological substrates against which to test potential mechanistic pathways between SES and cognitive and health outcomes. Of note, the results presented here do not establish a direct causal pathway between SES and brain

development, nor do they indicate that childhood SES exerts a deterministic effect on development. Rather, by resolving neuroanatomical substrates that vary closely with SES, we contribute new biological information to a growing field of multidisciplinary research that ultimately aims to reduce SES variation in health and achievement.

549 **References**

550 Ad-Dab'bagh Y, Einarson D, Lyttelton O, Muehlboeck J-S, Mok K, Ivanov O, Vincent RD, Lepage
551 C, Lerch J, Fombonne E, Evans AC (2006) The CIVET image-processing environment: A
552 fully automated comprehensive pipeline for anatomical neuroimaging research. In:
553 Proceedings of the 12th Annual Meeting of the Organization for Human Brain Mapping
554 (Corbetta M, ed). Florence, Italy.
555 Boca SM, Sampson JN (2014) Testing multiple biological mediators simultaneously.
556 Bioinformatics 30:214–220.
557 Brito NH, Noble KG (2014) Socioeconomic status and structural brain development. Front
558 Neurosci 8 Available at: https://www.ncbi.nlm.nih.gov/pmc/articles/PMC4155174/
559 [Accessed June 7, 2018].
560 Brooks-Gunn J, Duncan GJ (1997) The effects of poverty on children. Future Child 7:55–71.
561 Chakravarty MM, Bertrand G, Hodge CP, Sadikot AF, Collins DL (2006) The creation of a brain
562 atlas for image guided neurosurgery using serial histological data. NeuroImage 30:359–
563 376.
564 Chakravarty MM, Steadman P, van Eede MC, Calcott RD, Gu V, Shaw P, Raznahan A, Collins DL,
565 Lerch JP (2013) Performing label-fusion-based segmentation using multiple
566 automatically generated templates. Hum Brain Mapp 34:2635–2654.
567 Cocosco CA, Zijdenbos AP, Evans AC (2003) A fully automatic and robust brain MRI tissue
568 classification method. Med Image Anal 7:513–527.
569 Collins DL, Neelin P, Peters TM, Evans AC (1994) Automatic 3D intersubject registration of MR
570 volumetric data in standardized Talairach space. J Comput Assist Tomogr 18:192–205.

571 Draganski B, Kherif F, Klöppel S, Cook PA, Alexander DC, Parker GJM, Deichmann R, Ashburner J,
572 Frackowiak RSJ (2008) Evidence for segregated and integrative connectivity patterns in
573 the human basal ganglia. J Neurosci 28:7143–7152.
574 Duncan GJ, Magnuson K (2012) Socioeconomic status and cognitive functioning: Moving from
575 correlation to causation. Wiley Interdiscip Rev Cogn Sci 3:377–386.
576 Farah MJ (2017) The neuroscience of socioeconomic status: Correlates, causes, and
577 consequences. Neuron 96:56–71.
578 Farah MJ, Shera DM, Savage JH, Betancourt L, Giannetta JM, Brodsky NL, Malmud EK, Hurt H
579 (2006) Childhood poverty: Specific associations with neurocognitive development. Brain
580 Res 1110:166–174.
581 Gianaros PJ, Kuan DC-H, Marsland AL, Sheu LK, Hackman DA, Miller KG, Manuck SB (2017)
582 Community socioeconomic disadvantage in midlife relates to cortical morphology via
583 neuroendocrine and cardiometabolic pathways. Cereb Cortex 27:460–473.
584 Giedd JN, Blumenthal J, Jeffries NO, Castellanos FX, Liu H, Zijdenbos A, Paus T, Evans AC,
585 Rapoport JL (1999) Brain development during childhood and adolescence: A longitudinal
586 MRI Study. Nat Neurosci 2:861–863.
587 Hair NL, Hanson JL, Wolfe BL, Pollak SD (2015) Association of child poverty, brain development,
588 and academic achievement. JAMA Pediatr 169:822–829.
589 Hanson JL, Hair N, Shen DG, Shi F, Gilmore JH, Wolfe BL, Pollak SD (2013) Family poverty affects
590 the rate of human infant brain growth. PLoS ONE 8.
591 Hill WD, Hagenaars SP, Marioni RE, Harris SE, Liewald DCM, Davies G, Okbay A, McIntosh AM,
592 Gale CR, Deary IJ (2016) Molecular Genetic Contributions to Social Deprivation and

593 Household Income in UK Biobank. Curr Biol 26:3083–3089.
594 Hollingshead AB (1957) Two factor index of social position.
595 Holz NE, Boecker R, Hohm E, Zohsel K, Buchmann AF, Blomeyer D, Jennen-Steinmetz C,
596 Baumeister S, Hohmann S, Wolf I, Plichta MM, Esser G, Schmidt M, Meyer-Lindenberg A,
597 Banaschewski T, Brandeis D, Laucht M (2015) The long-term impact of early life poverty
598 on orbitofrontal cortex volume in adulthood: Results from a prospective study over 25
599 years. Neuropsychopharmacology 40:996–1004.
600 Jednoróg K, Altarelli I, Monzalvo K, Fluss J, Dubois J, Billard C, Dehaene-Lambertz G, Ramus F
601 (2012) The Influence of Socioeconomic Status on Children's Brain Structure. PLoS ONE 7.
602 Jones EG (1985) The Thalamus. New York: Plenum Press.
603 Kendler KS, Turkheimer E, Ohlsson H, Sundquist J, Sundquist K (2015) Family environment and
604 the malleability of cognitive ability: A Swedish national home-reared adopted-away
605 cosibling control study. Proc Natl Acad Sci 112:4612–4617.
606 Kim D-J, Park B, Park H-J (2013a) Functional connectivity-based identification of subdivisions of
607 the basal ganglia and thalamus using multilevel independent component analysis of
608 resting state fMRI. Hum Brain Mapp 34:1371–1385.
609 Kim P, Evans GW, Angstadt M, Ho SS, Sripada CS, Swain JE, Liberzon I, Phan KL (2013b) Effects of
610 childhood poverty and chronic stress on emotion regulatory brain function in adulthood.
611 Proc Natl Acad Sci 110:18442–18447.
612 Lawson GM, Duda JT, Avants BB, Wu J, Farah MJ (2013) Associations between children's
613 socioeconomic status and prefrontal cortical thickness. Dev Sci 16:641–652.
614 Lerch JP, Carroll JB, Spring S, Bertram LN, Schwab C, Hayden MR, Henkelman RM (2008)

615 Automated deformation analysis in the YAC128 Huntington disease mouse model.
616 NeuroImage 39:32–39.
617 LeWinn KZ, Sheridan MA, Keyes KM, Hamilton A, McLaughlin KA (2017) Sample composition
618 alters associations between age and brain structure. Nat Commun 8:874.
619 Luby J, Belden A, Botteron K, Marrus N, Harms MP, Babb C, Nishino T, Barch D (2013) The
620 effects of poverty on childhood brain development: The mediating effect of caregiving
621 and stressful life events. JAMA Pediatr 167:1135–1142.
622 MacDonald D, Kabani N, Avis D, Evans AC (2000) Automated 3-D extraction of inner and outer
623 surfaces of cerebral cortex from MRI. NeuroImage 12:340–356.
624 Mackey AP, Finn AS, Leonard JA, Jacoby Senghor DS, West MR, Gabrielli CFO, Gabrieli JDE
625 (2015) Neuroanatomical correlates of the income achievement gap. Psychol Sci 26:925–
626 933.
627 McDermott C (2018) Vertex-wise neuroanatomical change associations with childhood
628 socioeconomic status. figshare. https://doi.org/10.6084/m9.figshare.7089185.v2
629 McLoyd VC (1998) Socioeconomic disadvantage and child development. Am Psychol 53:185–
630 204.
631 Noble KG et al. (2015) Family income, parental education and brain structure in children and
632 adolescents. Nat Neurosci 18:773–778.
633 Noble KG, Houston SM, Kan E, Sowell ER (2012) Neural correlates of socioeconomic status in
634 the developing human brain. Dev Sci 15:516–527.
635 Noble KG, McCandliss BD, Farah MJ (2007) Socioeconomic gradients predict individual
636 differences in neurocognitive abilities. Dev Sci 10:464–480.

637 Pinheiro J, Bates D, DebRoy S, Sarkar D, R Core Team (2016) nlme: Linear and nonlinear mixed
638 effects models. R Package Version 31-128.
639 Raznahan A, Lenroot R, Thurm A, Gozzi M, Hanley A, Spence SJ, Swedo SE, Giedd JN (2013)
640 Mapping cortical anatomy in preschool aged children with autism using surface-based
641 morphometry. NeuroImage Clin 2:111–119.
642 Raznahan A, Shaw P, Lalonde F, Stockman M, Wallace GL, Greenstein D, Clasen L, Gogtay N,
643 Giedd JN (2011) How does your cortex grow? J Neurosci 31:7174–7177.
644 Raznahan A, Shaw PW, Lerch JP, Clasen LS, Greenstein D, Berman R, Pipitone J, Chakravarty
645 MM, Giedd JN (2014) Longitudinal four-dimensional mapping of subcortical anatomy in
646 human development. Proc Natl Acad Sci 111:1592–1597.
647 Redgrave P, Rodriguez M, Smith Y, Rodriguez-Oroz MC, Lehericy S, Bergman H, Agid Y, DeLong
648 MR, Obeso JA (2010) Goal-directed and habitual control in the basal ganglia:
649 implications for Parkinson's disease. Nat Rev Neurosci 11:760–772.
650 Reiss F (2013) Socioeconomic inequalities and mental health problems in children and
651 adolescents: A systematic review. Soc Sci Med 90:24–31.
652 Ritsher JE, Warner V, Johnson JG, Dohrenwend BP (2001) Inter-generational longitudinal study
653 of social class and depression: a test of social causation and social selection models. Br J
654 Psychiatry Suppl 40:s84-90.
655 Shackman AJ, Salomons TV, Slagter HA, Fox AS, Winter JJ, Davidson RJ (2011) The integration of
656 negative affect, pain and cognitive control in the cingulate cortex. Nat Rev Neurosci
657 12:154–167.
658 Sirin SR (2005) Socioeconomic status and academic achievement: A meta-analytic review of

research. Rev Educ Res 75:417–453.

Sled JG, Zijdenbos AP, Evans AC (1998) A nonparametric method for automatic correction of intensity nonuniformity in MRI data. IEEE Trans Med Imaging 17:87–97.

Tiikkaja S, Sandin S, Hultman CM, Modin B, Malki N, Sparén P (2016) Psychiatric disorder and work life: A longitudinal study of intra-generational social mobility. Int J Soc Psychiatry 62:156–166.

Tingley D, Yamamoto T, Hirose K, Keele L, Imai K (2014) mediation: R package for causal mediation analysis. J Stat Softw 59:1–38.

Trzaskowski M, Harlaar N, Arden R, Krapohl E, Rimfeld K, McMillan A, Dale PS, Plomin R (2014) Genetic influence on family socioeconomic status and children's intelligence. Intelligence 42:83–88.

Van Der Werf YD, Tisserand DJ, Visser PJ, Hofman PAM, Vuurman E, Uylings HBM, Jolles J (2001) Thalamic volume predicts performance on tests of cognitive speed and decreases in healthy aging: A magnetic resonance imaging-based volumetric analysis. Cogn Brain Res 11:377–385.

Vannest J, Karunanayaka PR, Schmithorst VJ, Szafkarski JP, Holland SK (2009) Language networks in children: Evidence from functional MRI studies. Am J Roentgenol 192:1190–1196.

Walhovd KB et al. (2016) Neurodevelopmental origins of lifespan changes in brain and cognition. Proc Natl Acad Sci 113:9357–9362.

Watt NF (1976) Two-factor index of social position: Amherst modification.

Wechsler D (1999) Wechsler abbreviated scale of intelligence. N Y Psychol Corp.

681 Wood SN (2011) Fast stable restricted maximum likelihood and marginal likelihood estimation
682 of semiparametric generalized linear models. J R Stat Soc Ser B Stat Methodol 73:3–36.
683 Xie Y, Chen YA, De Bellis MD (2012) The relationship of age, gender, and IQ with the brainstem
684 and thalamus in healthy children and adolescents: A magnetic resonance imaging
685 volumetric study. J Child Neurol 27:325–331.
686 Yarkoni T, Poldrack RA, Nichols TE, Van Essen DC, Wager TD (2011) Large-scale automated
687 synthesis of human functional neuroimaging data. Nat Methods 8:665–670.
688 Zijdenbos AP, Forghani R, Evans AC (2002) Automatic “pipeline” analysis of 3-D MRI data for
689 clinical trials: Application to multiple sclerosis. IEEE Trans Med Imaging 21:1280–1291.
690

691 **Tables**

692 **Table 1.** Participant Characteristics

Characteristic	Data
No. of individuals	623
No. of scans	1243
Sex, no.	
Female	299
Male	324
Age at first scan, years	
Mean (SD)	12.0 (4.0)
Range	5.2 – 25.4
Handedness, no.	
Left	35
Right	537
Mixed	51
Race, no.	
White	534
Black	40
Asian	14
Hispanic	20
Other	15
IQ	
Mean (SD)	114 (12.4)
Range	78 – 150
Hollingshead SES	
Mean (SD)	41.2 (18.3)
Range	95 – 20
No. of scans per individual, no.	
1 scan	279
2 scans	168
≥ 3 scans	176

693

	Model [A] Anatomy ~ β_{1A}(SES) + age + sex		Model [B] Anatomy ~ β_{1B}(SES) + β_{2B}(IQ) + age + sex			
Global Anatomical Metric	β_{1A} (SE)	p_{1A}	β_{1B} (SE)	p_{1B}	β_{2B} (SE)	p_{2B}
Total brain volume (cm^3)	1217.0 (263.0)	< 0.001	872.3 (268.3)	0.001	1645.8 (353.9)	< 0.001
Grey matter volume (cm^3)	773.6 (168.1)	< 0.001	539.7 (171.1)	0.002	1115.2 (226.6)	< 0.001
White matter volume (cm^3)	444.3 (117.6)	< 0.001	331.1 (121.2)	0.007	538.1 (159.8)	< 0.001
Cortical volume (cm^3)	642.4 (135.3)	< 0.001	458.5 (137.8)	0.001	876.7 (182.6)	< 0.001
Total surface area (cm^2)	144.1 (31.1)	< 0.001	111.6 (31.9)	< 0.001	156.0 (41.7)	< 0.001
Mean cortical thickness (cm)	0.00086 (0.00034)	0.0127	0.00047 (0.00035)	0.186	0.0018 (0.0005)	< 0.001
Hippocampus volume (cm^3)	3.56 (1.08)	0.001	2.58 (1.12)	0.022	4.59 (1.54)	0.003
Amygdala volume (cm^3)	1.22 (0.51)	0.018	0.87 (0.53)	0.10	1.64 (0.74)	0.027
Thalamus volume (cm^3)	9.10 (2.21)	< 0.001	6.89 (2.29)	0.003	10.44 (3.11)	< 0.001
Striatum volume (cm^3)	7.72 (3.76)	0.042	4.78 (3.89)	0.22	13.94 (5.07)	0.006
Pallidum volume (cm^3)	0.72 (0.57)	0.21	0.41 (0.59)	0.49	1.47 (0.80)	0.067

694

695 **Table 2.** Associations between SES and measures of cortical and subcortical anatomy.

696 Covariates in both models [A] and [B] include sex, centered age, and each individual's ID and

697 family ID.

Region of peak vertex	*t*	MNI coordinates			Top Neurosynth terms
		x	y	z	
Surface Area					
R postcentral gyrus	4.7	27	-35	72	Motor; Movement; Somatosensory; Execution; Motor Imagery
R orbitofrontal cortex	4.6	20	19	-22	Emotion; Reward; Affective; Fear; Regulation
L occipital pole	4.6	-35	-85	7	Visual; Objects; Motion; Orthographic; Reading
L inferior parietal cortex	4.6	-44	-38	49	Execution; Motor; Movement; Working Mem.; Spatial
L anterior cingulate gyrus	4.4	-4	36	10	Default Mode (DM); Reward; Self Referential; Emotional; Autobiographical
L middle temporal gyrus	4.3	-63	-43	-17	Semantic; Retrieval; Word; Mem.; Sentence
L precuneus	3.9	-4	-59	29	DM; Theory of Mind; Self Referential; Autobiographical Mem.; Mem. Retrieval
R middle temporal gyrus	3.5	61	-42	-10	Semantic; Language; Comprehension; Sentence; Word
R precuneus	3.4	4	-68	28	DM; Autobiographical Mem.; Mem. Retrieval; Self Referential; Episodic Mem.
R superior frontal gyrus	3.4	5	62	-5	DM; Autobiographical Mem.; Self Referential; Social; Theory of Mind
Cortical Thickness					
R supramarginal gyrus	4.3	59	-19	33	Somatosensory; Motor; Tactile; Movement; Pain

698

699 **Table 3.** Locations of peak SES associations with cortical morphology and top functional

700 associations as indicated by Neurosynth.

Figure Captions

Figure 1. Main effects of SES on global and local anatomy, after controlling for age and sex. (A) Standardized effect size of SES on each global cortical and subcortical brain measure estimated using scaled variables: total brain volume (TBV); grey matter volume (GMV); white matter volume (WMV); cortical volume (CV); total cortical surface area (SA); mean cortical thickness (CT); hippocampus volume; amygdala volume; thalamus volume; striatum volume; and pallidum volume. (B) Cortical surface regions that show a significant positive association with childhood SES. (C) Subcortical surface regions that show a significant positive association with childhood SES.

Figure 2. (A) Correlation between childhood SES and Full-Scale IQ in cross-sectional sample of 623 individuals, $r(621) = 0.31$, $p < 0.001$. (B) Map of main effects of SES and IQ on cortical surface area. Significant SES main effect is represented in red, IQ main effect in blue, and overlapping main effects in purple. Together, these main effects resemble the map of main SES effects on cortical SA without IQ as a covariate (Figure 1B). (C) A mediation analysis including surface area at each vertex as a separate mediator revealed regions of the left hemisphere that significantly mediate the relationship between SES and IQ.

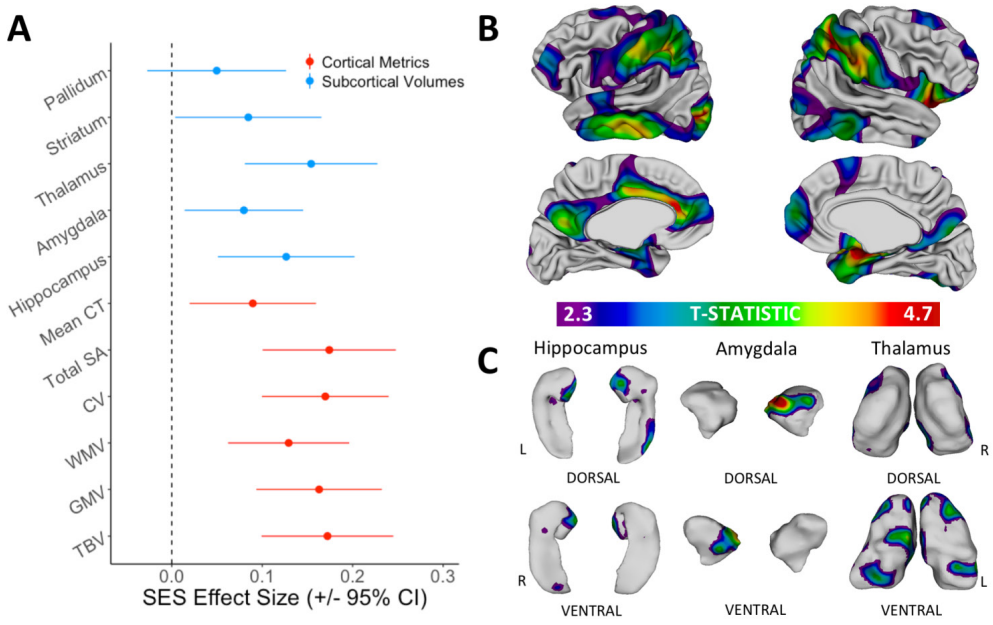

720

721

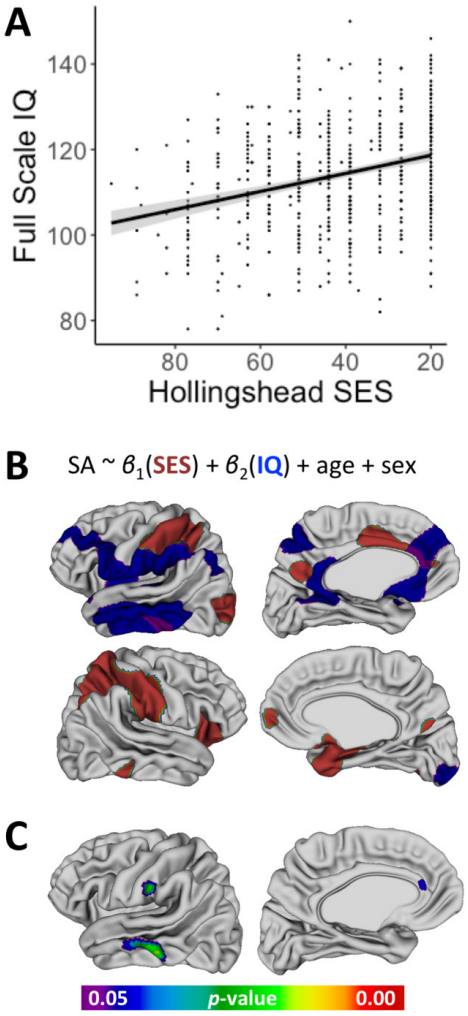

722